ANNALS OF GEOPHYSICS, 68, 5, DM581, 2025; doi:10.4401/ag-9217
OPEN ACCESS

Spatiotemporal evolution of broadband seismological networks in the Netherlands and the added value of the NARS-DICTUM array

Stephen Akinremi[*,1], Islam Fadel[1], Arie van Wettum[2], Elmer Ruigrok[2,3], Christine Thomas[4,5], Mark van der Meijde[1]

(1) Faculty of Geo-Information Science and Earth Observation (ITC), University of Twente, Enschede, The Netherlands
(2) Department of Earth Sciences, Utrecht University, Utrecht, The Netherlands
(3) Royal Netherlands Meteorological Institute (KNMI), De Bilt, The Netherlands
(4) Institute of Geophysics, University of Münster, Münster, Germany
(5) Geological Survey of Denmark and Greenland, Copenhagen, Denmark

Article history: received December 5, 2024; accepted May 4, 2025

Abstract

Passive seismic networks play critical roles in both seismicity monitoring and subsurface imaging. The seismic network in the Netherlands has continuously been expanded, both to monitor induced seismicity related to gas exploitation in the north and to monitor natural (tectonic related) earthquakes in the south of the country. Aside monitoring seismicity, the data delivered by the seismological networks is required for imaging the subsurface to improve our knowledge of the composition and structure. This serves as a crucial layer of information for decision-makers in regional planning, locating resources, and risk assessment regarding current and future projects utilising the Dutch subsurface. Over the years, there has been an increase in the number of geophones and accelerometers for monitoring mostly the high frequency seismic signals (induced seismicity) and imaging the near surface structure. However, the network of broadband seismometers for measuring tectonic events (usually lower frequency signals) and imaging deep subsurface is still limited. We describe an overview of previous temporary and permanent broadband seismometer deployments in the Netherlands, with a focus on the latest NARS-DICTUM array of 25 broadband seismometers, underscoring its design, instruments, installation, and some preliminary subsurface information delivered by the network.

Keywords: Seismological networks; Netherlands; Broadband; Seismicity monitoring; NARS-DICTUM; Subsurface imaging

1. Introduction

The Netherlands was among the first countries in the world to record earthquakes using seismometers, with its first seismometer installed in 1904 in De Bilt (KNMI, 2024) by the Royal Netherlands Meteorological Institute (KNMI), the national organization for monitoring seismicity in the Netherlands. In the Netherlands,

seismicity has been attributed to two main sources: induced and natural earthquakes (Fig. 1). Since 1986, there have been occurrences of earthquakes attributed to gas exploitation (KNMI, 2024). The KNMI operates a network of borehole geophones (since 1991) and surface accelerometers (since 1996) to measure earthquakes with magnitude greater than 2.0 throughout the Netherlands and magnitude greater than 1.5 in regions with mining activities. Since 2015, the network has been densified in areas with specific mining activities and can detect earthquakes lower than 1.5 magnitude (Ruigrok et al., 2023). For example, in North and South Netherlands, where there are small gas fields and geothermal fields, earthquakes from 1.0 magnitude can be measured. In Northeast Netherlands (Groningen), where there are large gas fields, earthquakes as low as 0.5 magnitude can be measured (Ruigrok et al., 2023).

Most of the natural (tectonic related) earthquakes in the Netherlands are concentrated in the Southern part (Limburg), especially in the Roer Valley Graben (RVG) (Dost and Haak, 2007). The RVG is a part of the active Lower Rhine Graben, which is a north-western extension of the Rhine Rift System (Dost and Haak, 2007). The RVG is bounded by two major active faults to which the major earthquakes are associated: the Feldbiss Fault to the southwest and the Peel Boundary Fault to the northeast (Dost and Haak, 2007; Houtgast and van Balen, 2000). Movements of these faults due to tectonic forces at the edges of the Eurasian Plate cause several earthquakes each year (Dost and Haak, 2007). The most powerful instrumentally recorded earthquake, with magnitude of 5.8 on the Richter scale, occurred near Roermond on 13 April 1992. For effective monitoring and accurate determination of source parameters or ground motion of large earthquakes with magnitudes greater than 3.5 (natural earthquakes or large induced earthquakes), broadband seismometer arrays are essential. This is because large magnitude earthquakes are associated with low-frequency motions to which geophones (typically in 1-15 Hz corner frequencies) and accelerometers are not sensitive. Broadband seismometers can typically record as low frequency at 8.33 mHz (120 seconds) up to 2.78 mHz (360 seconds) depending on the model. While there have been several permanent and temporary broadband seismometer deployments in the Netherlands, the space-time monitoring is still limited in resolution. Considering the earthquake occurrences and the proposed utilization of the Dutch subsurface for ultra-deep geothermal energy, carbon storage, and mining projects, a good monitoring network is essential.

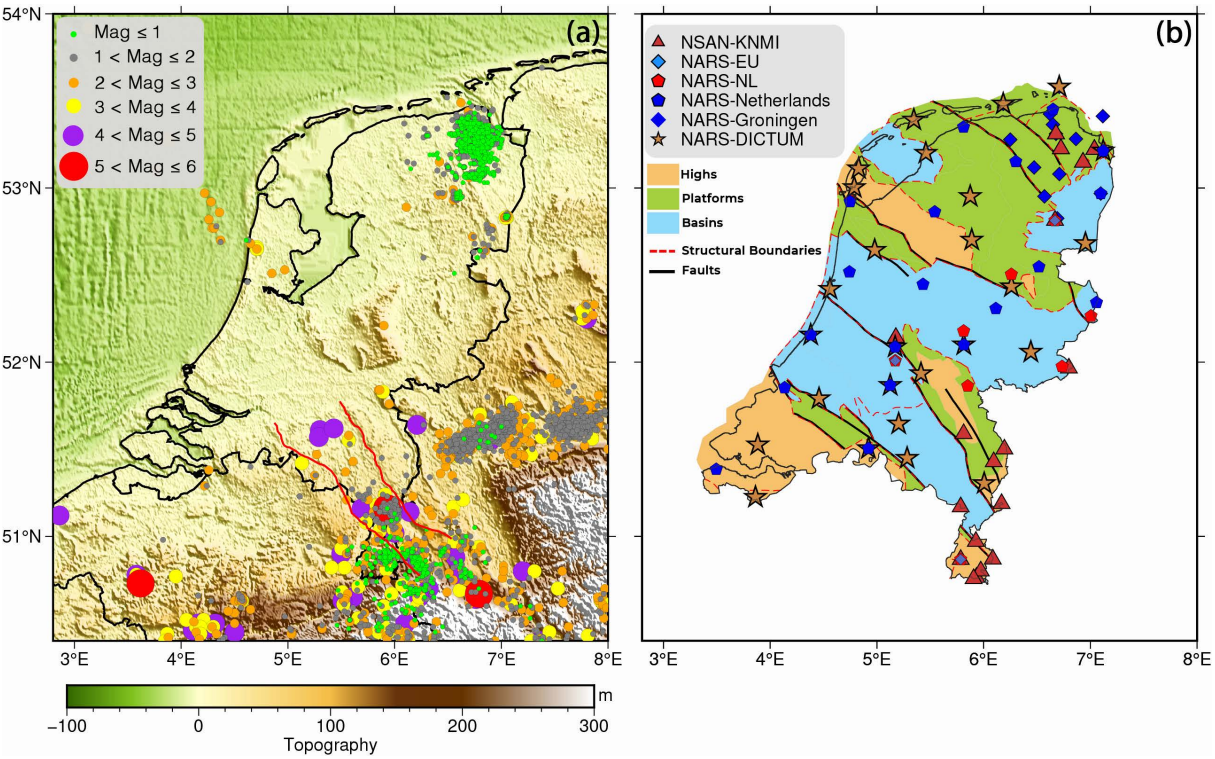

Figure 1. (a) Earthquake occurrence in and around the Netherlands from 1900 to 2024 retrieved from the KNMI catalogue (KNMI, 2025), showing the local magnitude and the epicentre of the earthquake and topography map as the base map. (b) Former and existing (temporary and permanent) broadband seismic network stations over several deployments with a tectonic map of the Netherlands (Kombrink et al., 2011) showing the major crustal structural elements as base map.

Aside monitoring seismicity, the data delivered by the seismological networks is essential for an improved knowledge of the composition and structure of the crust and the upper mantle. Such composition and structural models will also serve as a crucial layer of information for decision-makers in regional planning, locating resources, and risk assessment regarding current and future projects utilising the Dutch subsurface. The structure of the uppermost 3 km of the crust of the Netherlands has been well mapped using active seismic, short period passive seismic, and well log data (e.g. Kombrink et al., 2011). However, information about the deep crustal structure, beyond 3 km, is limited and poorly constrained. The latest crustal model of the Netherlands was presented by Yudistira et al. (2017), using ambient noise to derive crustal shear wave velocity. However, their shear wave velocity model has limited lateral resolution of ~50 km and no coverage at the coastlines and the northern parts of the Netherlands. For the upper mantle structure beneath the Netherlands, there is limited information available. It is therefore important to further utilise the existing data, as well as increase the broadband seismic network density to better image and understand the composition, tectonic settings and interactions between the subsurface structural elements.

From 2022, we deployed a Network of Autonomously Recording Seismographs (NARS) consisting of 25 broadband seismometers. This was a part of the "Deep, deeper, deepest NL-Imaging the Dutch crust and upper mantle using multi-geo-observables (DICTUM)" project. The NARS-DICTUM array aims to densify the existing network operated by the KNMI and complement previous temporary seismometer deployments in the Netherlands. This temporary NARS-DICTUM deployment is focused on seismicity monitoring and high-resolution imaging of the deep subsurface beneath the Netherlands. In Section 2 of this paper, we evaluate the capacity of the broadband seismic monitoring network in the Netherlands from previous temporary and permanent deployments. In Section 3, we focus on the current NARS-DICTUM inland array deployment, instruments, its design, development, installation, and some preliminary subsurface information delivered by the network.

2. Previous Temporary and Permanent Seismological (Broadband) Data Campaigns in the Netherlands

In this section, we describe the previous temporary and permanent broadband seismometer deployments in the Netherlands, which are the Netherlands Seismic and Acoustic Network (NSAN) and the past NARS deployments.

2.1 The Netherlands Seismic and Acoustic Network (NSAN)-NL

The KNMI operates the NSAN-NL network which currently comprises of 15 permanent broadband stations, which are mainly concentrated in the southeast of the Netherlands, where most of the tectonics-related seismicity occurs (Fig. 2; KNMI, 1993). This network serves as a baseline for seismic monitoring in the Netherlands. Digitized data are available from 1993. The network's focus on the southeastern and northeastern regions means that little or no broadband seismic data are available in other regions of the Netherlands. Figure 2 shows how the NSAN-NL stations in operation from 1980 spatially correlate with earthquake events until now. After 2012, the network was slightly extended to partially cover the Groningen region in the northeastern region of the Netherlands (Fig. 2c, d).

2.2 Network of Autonomously Recording Seismographs (NARS)

The NARS array has deployed broadband seismometers in the Netherlands and western Europe in 4 previous data campaigns. In the following subsections, we describe these 4 NARS arrays.

2.2.1 NARS-Europe Array

The NARS-Europe array consisted of 18 stations deployed from 1983 to 1987 in Netherlands, Belgium, France, Spain, Denmark, and Sweden (Nolet and Vlaar, 1982; Utrecht University – UU Netherlands, 1983). The array aimed at imaging the deep subsurface structure in western Europe.

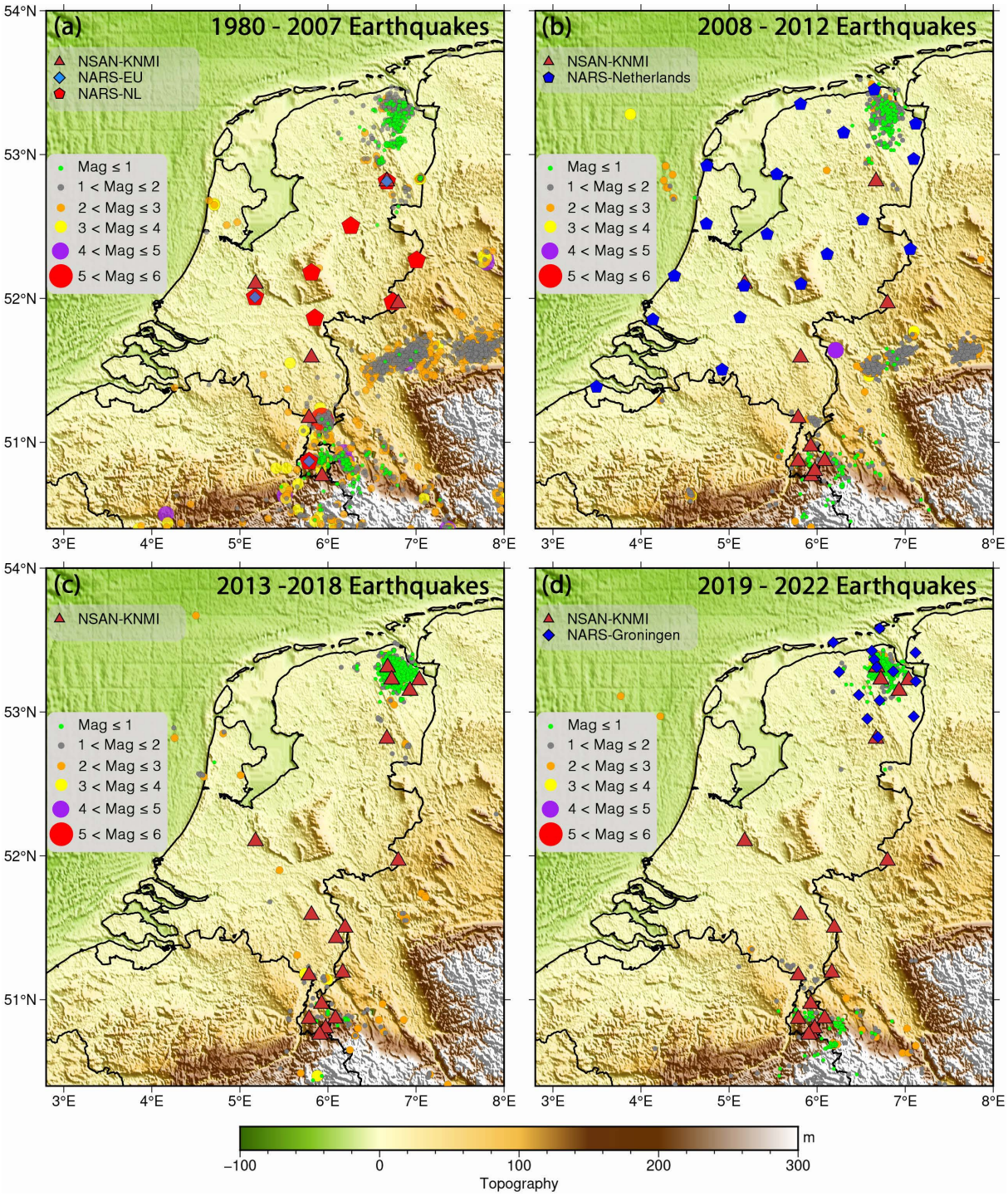

Figure 2. Earthquake occurrences maps for different time intervals (a) 1980-2007; (b) 2008- 2012; (c) 2013-2018; and (d) 2019-2022; with corresponding broadband seismometer stations recording within those periods.

2.2.2 NARS-NL Array

The NARS-NL (1989-1992) array consisted of 14 stations in Netherlands, Germany and Belgium (Utrecht University – UU Netherlands, 1983). The array recorded the 5.8 magnitude Roermond earthquake of April 13th, 1992, in the Netherlands. The data from the array facilitated the determination of the epicentre (in RVG), focal depth, focal mechanism, and origin time of the event (Paulssen et al., 1992). Aside this, the array also provided some first insight into the deep crustal structure beneath the Netherlands, including some earliest crustal thickness estimates (Paulssen et al., 1993; Visser and Paulssen, 1993).

2.2.3 NARS-Netherlands Array

NARS-Netherlands is a network of 19 seismometers deployed across the Netherlands (Utrecht University – UU Netherlands, 1983; Yudistira et al., 2017). The network was a temporary deployment that recorded from 2008 to 2012 and included a permanent station (since 1983) in Utrecht. The NARS-NL deployment increased the lateral resolution of the seismometer network in the Netherlands to ~50 km (Fig. 2b). Yudistira et al. (2017) delivered the first crustal shear wave velocity model of the Netherlands using ambient noise field from the data delivered from the NARS-Netherlands stations and 13 other stations in and around the country.

2.2.4 NARS-Groningen Array

The NARS-Groningen seismological network of 14 broadband seismometers was deployed in Northeast Netherlands (Groningen area) to monitor subsurface changes related to gas production in the region (Fig. 2c). The temporary deployment ran from 2019 to 2022 and delivered valuable data for imaging and monitoring toward a better understanding of the subsurface dynamics related to gas production in the region (Fig. 2d).

3. NARS-Dictum Seismological Network, Data and Methods

The NARS-DICTUM broadband seismological deployment (Fig. 3) was initiated in 2022. The project aims to create new crust and upper mantle models of the Netherlands in high resolution with data from this deployment and previous data campaigns. The deployment densifies the existing seismological network with 25 inland seismometers (Fig. 3). There is a proposed deployment of 3 additional North-Sea Posthole Seismometers (NPS) as part of this project.

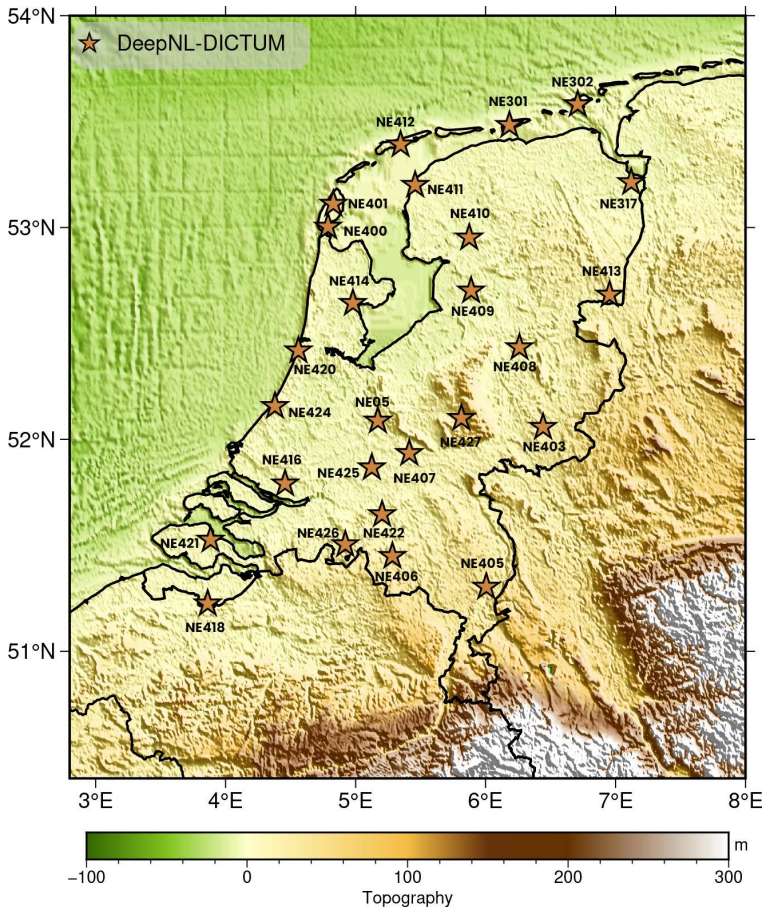

Figure 3. Location of NARS-DICTUM broadband stations.

The NPS deployment are being designed to ensure they can withstand the harsh conditions at the sea floor. The new NPS station design is temporarily deployed for testing and a full deployment is done at a later stage along the coastlines of the Netherlands. The current NARS-DICTUM inland broadband array complements the previous and currently active stations in the Netherlands. By integrating the new NARS-DICTUM and data from other deployments, a high-resolution coverage across the Netherlands can be achieved for subsurface imaging and supporting seismicity monitoring activities by KNMI. In the following subsections, we provide descriptions of the development and progress of the NARS-DICTUM deployment, and some preliminary results delivered by the new array.

3.1 Network Optimization and Site Selection

The station location and spacing were decided to complement the existing stations from NSAN-NL and to fill gaps not previously covered by NARS deployments (Fig. 3 and Table 1). A few stations from previous deployments could be retained and were incorporated into NARS-DICTUM. Spatial resolution tests were done to determine the most optimal station locations to retrieve high resolution subsurface information from the network. Figure 4 (f and i) shows the resolving capabilities of the new array in combination with other previous or current deployments in and around the Netherlands. The densified network can retrieve the velocity structure of ~25 km spatial resolution, as compared to the ~50 km (Fig. 4b) resolving capacity of the latest crustal velocity model of the Netherlands by Yudistira et al. (2017).

In the site selection for the surface seismometers, we considered the standards described by Trnkoczy et al. (2012). Appropriate sites should have low effects of cultural noise, good ground coupling, be safe, have the right permissions to use, and be accessible for installation and maintenance. We selected sites that are preferably more than 5 km offset from rail tracks and have lower sources of other cultural noise like human activities. We installed most stations in private farmlands that are not actively cultivated and at KNMI weather and borehole stations. All sites are far from main roads and, in the Dutch context, relatively quiet locations.

Station	Location	Sensor	Latitude	Longitude	Altitude	Installation Date
NE301	Schiermonnikoog	Trillium 120-PH	53.4833	6.1834	3	2019/08/14
NE302	Borkum (Germany)	Trillium 120-PH	53.5812	6.7079	3	2019/08/16
NE317	Finsterwolde	STS-2	53.2134	7.1196	0	2019/08/29
NE400	Den Burg	Trillium 120-PH	53.0036	4.7887	0	2022/07/26
NE401	De Cocksdorp	Trillium 120-PA	53.1114	4.8290	0	2022/07/15
NE403	Ruurlo	Trillium 120s Compact	52.0582	6.4418	18	2023/05/24
NE405	Helden	Trillium 120s Compact	51.3038	6.0045	34	2023/05/29
NE406	Vessem	Trillium 120-PH	51.4487	5.2827	27	2023/05/23
NE407	Zoelen	Trillium 120-PA	51.9353	5.4128	4	2022/09/08
NE408	Heino	Trillium 120-PH	52.4338	6.2615	3	2022/11/15
NE409	Marknesse	Trillium 120-PA	52.7019	5.8878	-4	2022/11/24

Station	Location	Sensor	Latitude	Longitude	Altitude	Installation Date
NE410	Oudehaske	Trillium 120-PA	52.9522	5.8744	0	2022/10/11
NE411	Wijnaldum	Trillium 120-PH	53.1995	5.4578	0	2022/11/29
NE412	Hoorn Terschelling	Trillium 120-PH	53.3912	5.3457	0	2022/11/30
NE413	Erica	Trillium 120-PH	52.6823	6.9536	13	2023/08/17
NE414	Berkhout	Trillium 120-PA	52.6427	4.9787	-3	2022/11/10
NE416	Westmaas	Trillium 120-PH	51.7909	4.4579	0	2023/06/08
NE418	Westdorpe	Trillium 120-PA	51.2251	3.8617	1	2022/11/03
NE420	Bloemendaal	Trillium 120-PH	52.4195	4.5604	3	2022/08/25
NE421	Wilhelminadorp	Trillium 120-PA	51.5260	3.8835	0	2022/11/07
NE422	Helvoirt	Trillium 120-PH	51.6462	5.2039	5	2023/07/26
NE424	Wassenaar	STS-2	52.1574	4.3794	0	2022/09/01
NE425	Herwijnen	STS-2	51.8666	5.1251	20	2022/09/5
NE426	Chaam	STS-2	51.5043	4.9209	10	2022/09/13
NE427	Otterlo	STS-2	52.1003	5.8145	15	2022/09/13

Table 1. The NARS-DICTUM Stations.

3.2 Instruments

The instrument setup for recording at each station consists of three-components broadband seismometer, a data logger, a GPS receiver, a GSM modem and power supply. We used Nanometric Trillium 120-PH and Streckeisen (STS-2) seismometers from the instrument pool of the Utrecht University and University of Twente. Additional Nanometric Trillium 120-PA and Trillium 120s compact from the Institute of Geophysics, University of Münster, Germany, were used.

The seismometers record ground motion in the vertical, north-south, and east-west directions with corner frequencies at 8.3 mHz and 150 Hz (120 s-0.0067 s) for Trillium 120-PA and 8.3 mHz and 100 Hz (120 s-0.01 s) for the other sensors. Between the two corner frequencies, the sensors have maximum and frequency independent sensitivity (i.e. a flat response) with respect to particle velocity. The seismometers are connected to the dataloggers that do Analog-to-Digital conversion, timing of the data, data processing, and internal data storage. We used Taurus data loggers for the Trillium 120-PA and Trillium 120s compact sensors, and Centaur data loggers for the Trillium 120-PH sensors. A data logger developed by Utrecht University was utilized for the STS-2 sensors. The GPS antenna ensures accurate timing of the data by synchronizing the internal clock of the data logger with the external GPS clock. Via the GSM modem, the data logger transmits daily data records to a local data center, enabling remote monitoring of the station's status via SMS. The data logger is connected to a power box for running the station. More details about the power supply will be discussed in the coming sections.

3.3 Site Preparation and Station Deployment

The station deployment techniques were designed to ensure good coupling and safety of the instruments. We had 3 major types of installation techniques for this array, which are based on the type of sensor and the location of the station. These techniques are described as follows.

1. **Deployment A: For Trillium 120-PA, Trillium 120s compact and STS-2 seismometers**

These three sensor types are horizontally leveled using three legs and require installation on hard underground for proper coupling. In the Netherlands, the topsoil usually consist of soft clay, sand or peat and the groundwater level

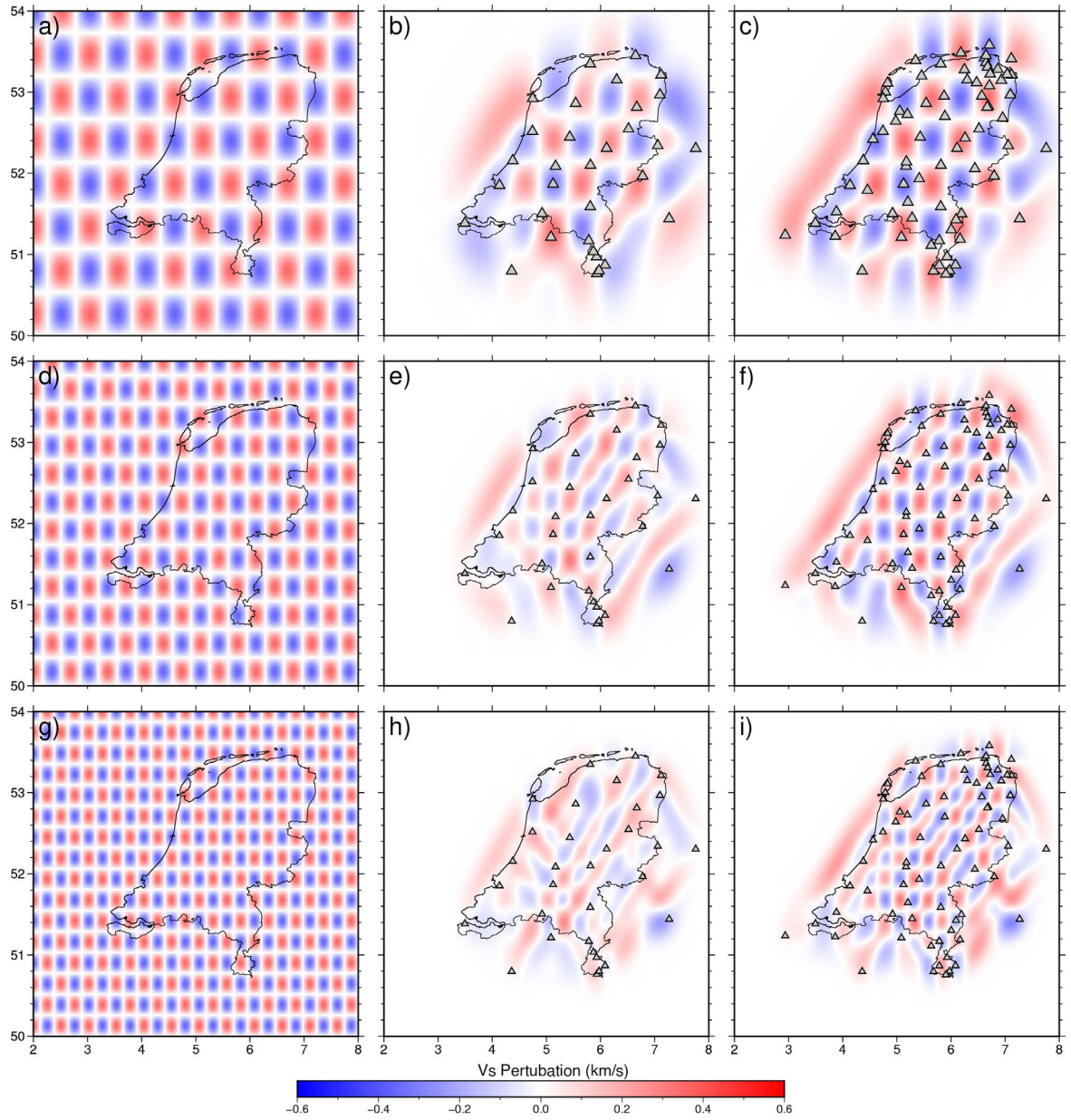

Figure 4. Resolution tests comparing the velocity anomaly sensitivity of the previous broadband seismological array with the newly densified network. Stations that are just across the borders of the Netherlands borders are included. The first column (a), (d), and (g) show the input velocity anomaly for checkerboard test with 0.5-, 0.33-, and 0.25-degree resolutions, respectively. The second column (b), (e), and (h) show the resolving capabilities of the data used to generate the shear wave velocity model of Yudistira et al. (2017), in the same resolution order 0.5, 0.33, and 0.25 degree as the first column. The third column (c), (f), and (i) show the resolving capabilities using the upgraded inland broadband network, in the same resolution order 0.5, 0.33, and 0.25 degree as the first column.

is usually high. Hence, we placed these sensors in PVC tubes and installed them in pits. The PVC tube is stabilized by gluing a waterproof ceramic tile to its base and the tile is placed in a bed of fast-setting cement in the pit. The pit is prepared to have a maximum depth of 0.75 m, and a hole is dug to access the main pit as in Fig. 5. This ensures that the adjustable feet of the sensor remain within reach. The sensor is connected to the data logger and adjusted in the tube to ensure it is leveled. The sensor is then covered with plastic bags of dry sand till the tube is three-quarters full, to ensure proper ground coupling. The data logger and GPS antenna are placed on top of the sandbags. Connection from the data logger to the power source outside the tube is done using a waterproof flexible hose. The tube is insulated at the top using insulation pearls, closed with a PVC lid and secured using a padlock chain. The PVC cover does not result in signal loss for the GPS antenna. Because of the weight of the sandbags and the protrusion of the tile at the base of the tube, the station installation cannot be pushed up by rising groundwater level. Moreover, sandbags improve the thermal isolation of the sensor, minimizing the effects of daily and seasonal temperature fluctuations.

2. Deployment B: For Trillium 120-PH seismometers

This sensor type is designed for simple and quick installation. We designed a metal watertight drill tube of length of 1.8 m with wide thread at the base to screw it to the ground (Fig. 6a). A pre-drilling is done with a 20 cm

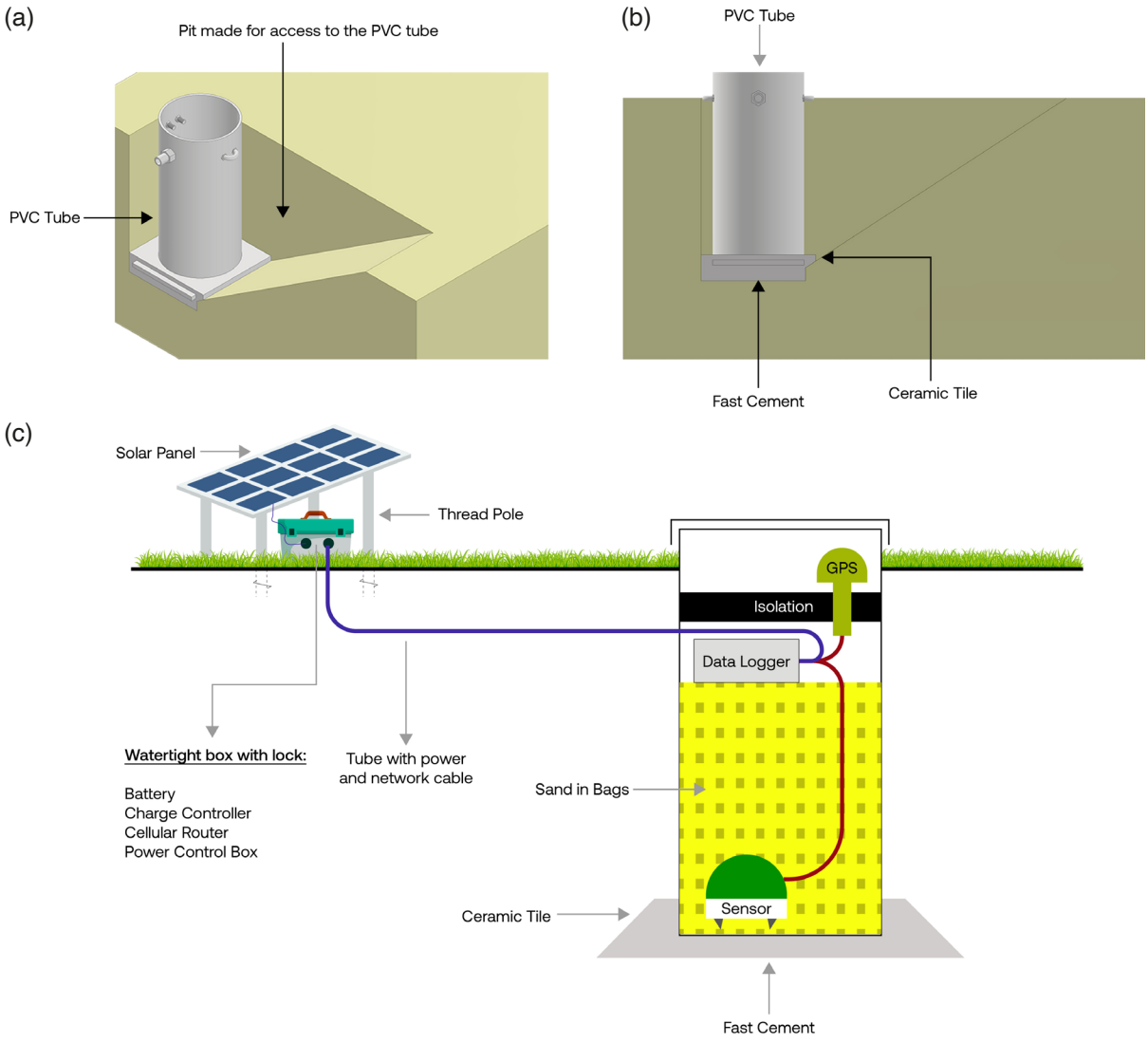

Figure 5. (a) Pit dug for the PVC to install the seismometer. The pit is widened on one side to ensure access to the PVC when placing, orienting and levelling the sensor. (b) Side view of the pit and PVC tube showing the ceramic tile and fast cement at the base of the tube. (c) Schematic showing the deployment design for Trillium 120-PA, Trillium 120s compact, and STS-2 seismometers in a PVC tube (including the data logger and GPS antenna) placed in a pit. The other components of the station are placed outside.

auger up to 1.7 m depth, after which the pipe is screwed into the ground with manual force using steel scaffolding. The seismometer, surrounded by sand, and data logger on top are placed in this tube. The wide thread, the weight of the seismometer and the sand ensure effective ground coupling while counteracting the upward buoyancy forces from the groundwater. The tube is covered with a metallic lid and safety padlocks. An insulation box is placed on it to minimize the effects of temperature fluctuation.

Another scenario for the Trillium 120-PH seismometers is directly burying the seismometers in the ground without the metal tube, which is a traditional posthole deployment (Fig. 6b). A pre-drill is done to a depth of 1 to 1.2 m with 20 cm auger, depending on the soil conditions. Then, sand is added to the hole bottom to prevent the sensor from being stuck in the soil. After that, the sensor is placed and levelled to guarantee a good vertical alignment. More sand is added to surround the sensor up to the top of the hole to ensure it will not get stuck in the (clayey) soil. The natural soil is then used to cover the top 10 cm to provide a natural view of the site and to allow the growth of vegetation. The sensor is connected to the datalogger, which is placed in a waterproof box containing the battery and the modem.

3. **Deployment C: For stations collocated with existing KNMI weather stations and boreholes**

Some of our stations are deployed in existing structures of KNMI weather and borehole stations. These structures have shelters and are well protected from the effects of weather. For the borehole stations, the sensor and the other components are placed within a plastic pod and covered with sand (Fig. 7a-d). For the weather station sites, all the components of the station, except the sensor and the GPS antenna, are placed in such shelters (Fig. 7e). The sensor is deployed using the previously described scenarios at 2-3 m distance from the shelter within the permitted zone of the KNMI station (Fig. 7e). The stations collocated with the KNMI sites have the advantage of the regular power supply reducing the overburden of solar panel installation.

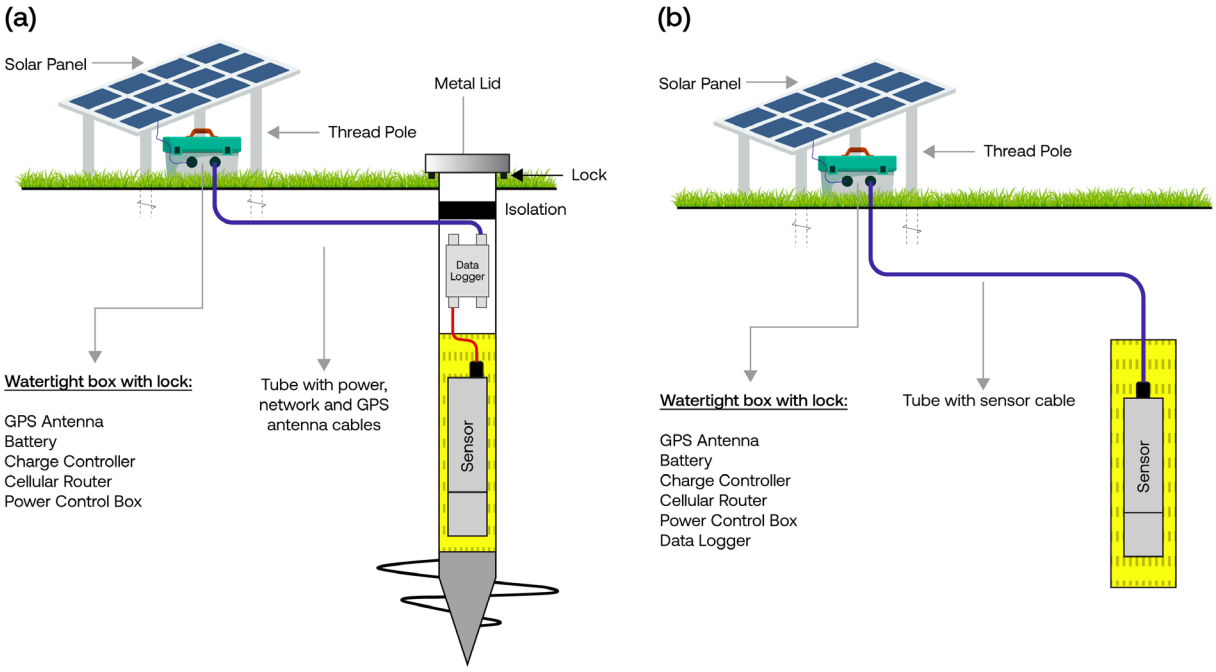

Figure 6. Schematic showing the deployment designs for the Trillium 120-PH (a) Scenario A: the seismometer and data logger are installed in a metal watertight drill tube that is screwed to the ground using wide threads. The other components of the stations, including the GPS antenna, are placed outside. (b) Scenario B: Traditional deployment design, where the seismometer is directly buried in the ground without the metal tube.

3.4 Site Preparation and Station Deployment Positioning and Orientation

A modified airplane gyrocompass is used in all seismometer deployments in combination with a highly sensitive normal compass. The traditional workflow is to find two or sometimes three nearby places that have a lower

apparent culture magnetic noise to identify the north direction using the highly sensitive compass. After declination correction, the gyro is used to store the north direction to double-check the accuracy of the north direction at the different sites. Once the north direction is confirmed in the two or three sites, depending on the site nature, the confirmed north direction is stored for the deployment of the station. To orient the Trillium 120-PA and Trillium 120s compact seismometers, we used a laser beam attached to the gyro compass to orient the seismometer N-S indicator correctly. This is because these two sensors are still accessible while already in the pit. For the Trillium 120-PH seismometer, we used a different technique to orient it, since the seismometer is not accessible after placing it in the tube. A specially constructed in-house adaptor is used to lower this sensor into the tube and orient it properly. The adaptor frame is exactly parallel with the N-S indicator of the sensor, and it is mounted using two long wire ends that fit in the sensor's existing holes. The frame of the adaptor is oriented with a gyro compass and when the sensor is properly positioned, the wires are loosened, and the adaptor is removed.

Figure 7. (a-d) Example of deployment of station NE411 in a KNMI Borehole location where the seismometer is placed in the existing safe facility and connected to electricity supply. All the components of the stations are placed in the instrument vault, except the GPS antenna, which is placed at the top for proper signal reception. (e) Example of deployment of station NE418 at a KNMI automatic weather station. The sensor is buried in a tube installation in the ground and covered with black plastic for visibility. Other components are connected to electricity supply and stored in the weather station.

3.5 Power

The power usage of each station is 1.8 Watt, on average, and it increases to 7 Watt when the cellular router is switched on for data sending or communication. An in-house power controller board is deployed to regulate power supply to the cellular router and data logger, optimizing energy consumption and ensuring continuous station operation. The power controller supplies power to the router for only 15 minutes at a fixed interval of 6 hours. During this power up, the data logger sends the latest data and status information to the data center. We used two different power sources – solar energy and grid power – for the stations, depending on the installation location. The stations deployed in farmland are independent of electricity supply and are powered by 133 W solar panels in combination with 80 Amp Hour battery. The batteries used in the deployments are maintenance free and have a long service life. A good quality Maximum Power Point Tracking charge controller is used to connect the solar panel to the battery to multiply the current and voltage to provide the maximum power at a given moment. To minimize noise from wind-induced vibrations, the solar panels are typically installed 2-3 m away from the sensor and tilted at an angle of 15° from the vertical to ensure that maximum sun energy is harvested in the winter. In December and January, when the angle of the sun shines for only a few hours a day at about 15° (at 52° latitude), this solar panel orientation improves efficiency. This ensures that the station keeps running throughout the winter period. For the stations collocated with KNMI weather and borehole stations, where the electricity supply is constant, we use direct AC electricity and AC to DC converters to charge the batteries through a charge controller. The setup design with the DC battery is utilized to guarantee that the station is operating even during periods of power cuts.

3.6 Communication and Data Streaming

We used a 4G/LTE Wi-Fi router to independently set up a Virtual Private Network (VPN) connection between the station and our data center server. The option of using SIM with fixed IP address is quite expensive in the Netherlands. Hence, we used a more cost-effective alternative with regular SIM. The regular SIM is used in combination with a 4G/LTE Wi-Fi router, which independently sets up a VPN client connection to our VPN server. This makes communication with the station possible remotely via SMS. It is also possible to log into the data logger remotely for station maintenance. Furthermore, daily recorded data is sent to the data server at the end of each day and important status information is sent by email. The communication and data streaming capabilities make station maintenance and data availability possible without site visits.

3.7 Ambient Seismic Noise Field in the Netherlands

We used the probabilistic power spectral density (PPSD) analysis to characterize ambient seismic noise levels in the Netherlands from the data delivered by selected stations from the NARS-DICTUM array. The PPSD is computed using the procedure from Mcnamara and Buland (2004). The PPSD of the vertical component of the ambient seismic velocity field of one month recording is shown for 4 stations in Fig. 8: 2 near the coastline (NE401 and NE416) and 2 farther inland (NE405 and NE413). One peak corresponding to the secondary microseism is observed on the PPSDs. The PPSDs are made for the month of August. In this time of year, the single-frequency microseism cannot be seen well from the Netherlands. The primary microseisms (or single frequency microseisms) are generated from the ocean gravity waves coupling with the slope of the coast (Hasselmann, 1963), while the secondary microseisms (or double frequency microseisms) are created from the interaction of ocean gravity waves travelling in opposite directions. Secondary microseisms are observed between the periods of 1-5 s (Fig. 8). The noise models of Peterson (1993) are compared with the PPSD plots (Fig. 8), revealing that noise levels in the Netherlands exceed the high noise model. This trend is observed for both stations near the coast with higher noise levels (NE416 and NE420) and for inland locations (NE405 and NE408). Similar high noise levels were observed by Yudistira (2015) in the data from the NARS-Netherlands array.

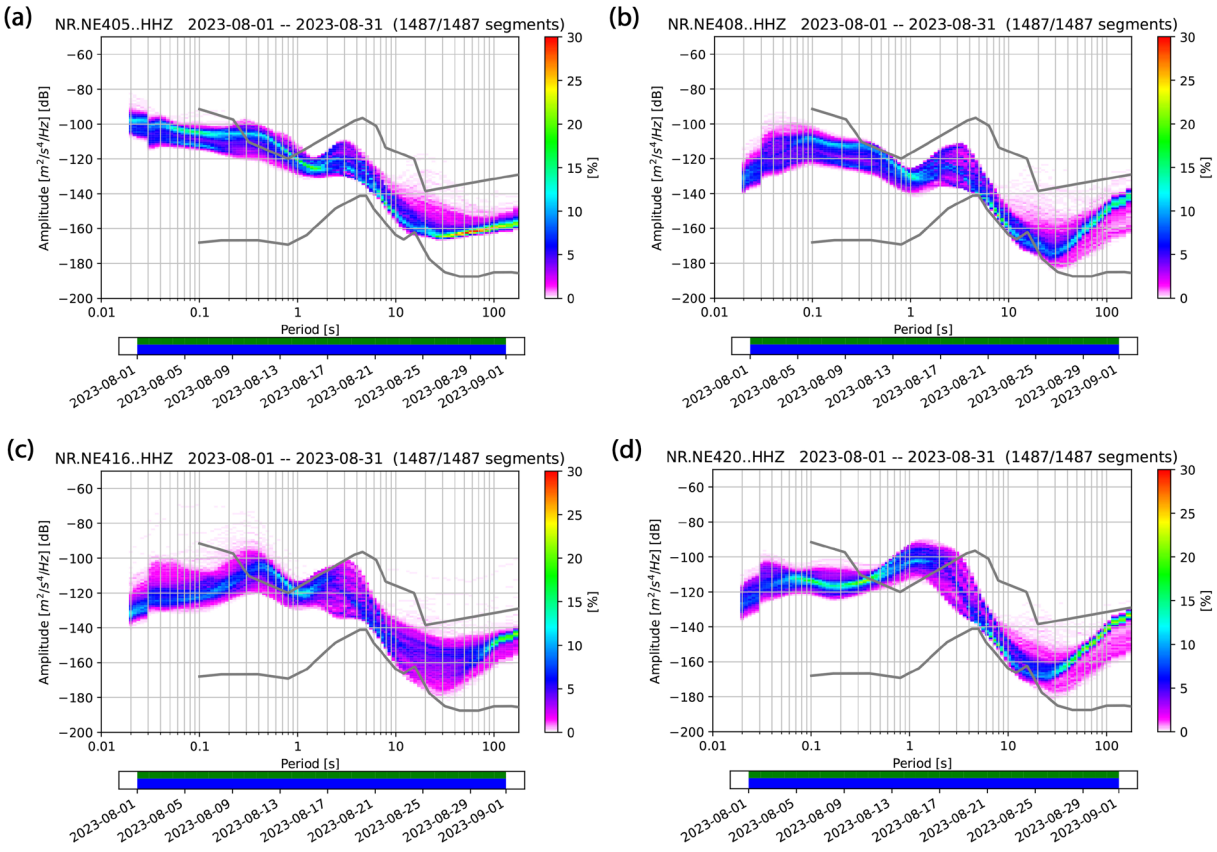

Figure 8. The average probabilistic power spectral density plot for a month recording (August 2023) for four stations (a) NE405; (b) NE408; (c) NE416; (d) NE420. The grey solid lines represent the high and low noise models of Peterson (1993).

3.8 H/V Spectral Ratios from the Ambient Seismic Field in the Netherlands

The Horizontal-to-Vertical Spectral Ratio (HVSR) analysis was done for the NARS-DICTUM stations to estimate local site response from the ambient seismic noise fields. The HVSR is derived by calculating the ratio of the Fourier amplitude spectra between the horizontal and vertical components of a seismic recording. We used the hvsrpy software of Vantassel (2020), which implements the automatic frequency-domain time window rejection algorithm of Cox et al. (2020). The characteristics of HVSR amplitude largely reflect the in situ lithostratigraphic sequences and indicate the presence of a significant velocity contrast near the surface. When a near surface velocity contrast is present, the peak in the HVSR curve corresponds closely to the site's shear-wave resonance frequency. The peak in the HVSR curve indicates the frequency at which the subsurface layers resonate, and this resonant frequency is typically related to the depth of a significant impedance contrast, such as between loose sediments and bedrock (e.g., Bonnefoy-Claudet et al., 2006). A HVSR peak at a low frequency, for example 0.1-1 Hz suggests a deep subsurface discontinuous layer beneath the station, as low frequencies penetrate deeper into the earth. This is common in stations over thick sedimentary basins (Bonnefoy-Claudet et al., 2006; Van Ginkel et al., 2022). A HVSR peak at higher frequency (1-10 Hz) indicates shallower discontinuous layer beneath the station and suggests that the bedrock or a similar strong impedance layer is closer to the surface. The amplitude of the HVSR peak reflects the magnitude of the impedance contrast between layers. A high HVSR peak (often >4) usually indicates a strong impedance contrast, such as from soft sediments overlying hard bedrock. A low HVSR peak or a flat HVSR curve suggests a gradual impedance change in the subsurface layers with depth. Figure 9 shows examples of HVSR of representative stations from different tectonic domains in the Netherlands. Flat HVSR curves with no distinguishable peaks are found for stations (NE302, NE410, NE408, NE420, NE427, NE403, NE422, NE406) where strong velocity contrasts are absent in the shallow subsurface. This indicates deep sedimentary basins with gradual velocity gradients between the layers. Some HVSR (NE401, NE405, NE407, NE411, NE413, NE418, NE424) show

significant peak amplitudes that correspond to the presence of velocity contrast beneath the stations. This distinct HVSR peak amplitudes can be interpreted as the presence of strong impedance contrast within the sedimentary basin, or shallow depth to bedrock. Van Ginkel et al. (2022) found similar distinct peaks from stations on structural highs in southeast Netherlands.

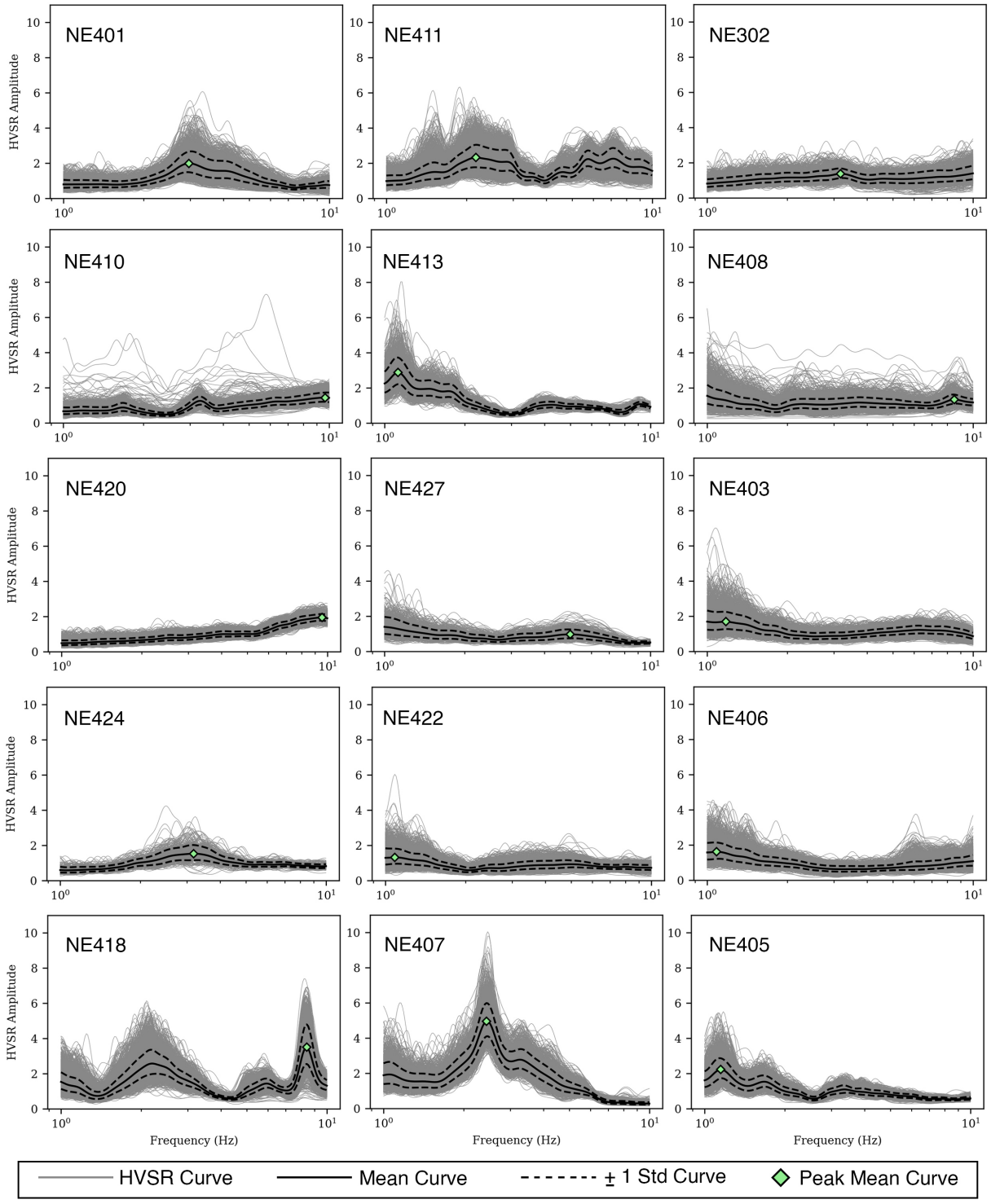

Figure 9. HVSR curves from ambient noise for 15 stations of the NARS-DICTUM network.

3.9 The Waveform of Elbistan 7.6 Mw Magnitude Earthquake of 6 February 2023 in Turkey

We assess the data quality of the Elbistan 7.6 Mw magnitude earthquake on 6 February 2023 in Turkey as recorded by the NARS-DICTUM array. The earthquake signal on the vertical component, as recorded by 10 of the stations in the array, is shown as a function of epicentral distance (Fig. 10). The array demonstrates high-quality data acquisition, with clear and well-defined seismic waveforms. A notable feature is the consistent phase shift observed between stations, which corresponds to the varying distances from the epicentre and heterogeneity in the local crustal structures at the stations. Another observation is the variation in the amplitudes of later phases that could be associated with complex crustal structure and variation in the attenuation of the seismic signals below the array, which would require a further investigation (Furumura and Kennett, 2001).

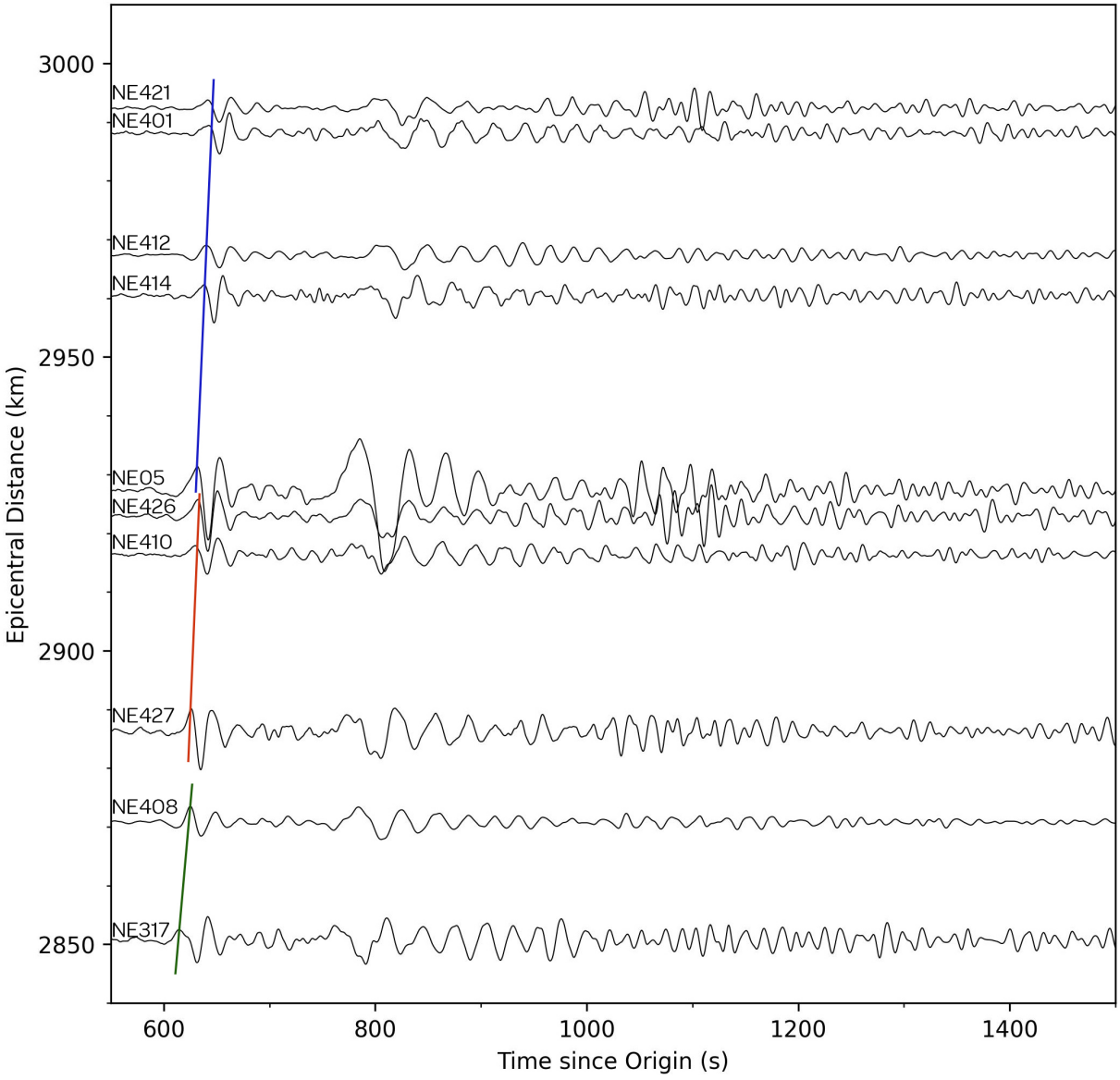

Figure 10. Vertical component seismograms of the 7.6 magnitude earthquake of 6th February 2023 in Turkey plotted as a function of the epicentral distance to some NARS-DICTUM stations.

4. Conclusions

We presented the space-time evolution of seismological networks in the Netherlands for seismicity monitoring and subsurface imaging, with a focus on broadband seismic networks. We provided a detailed description of the latest deployment, the NARS-DICTUM broadband array of 25 stations. The NARS-DICTUM array aims to densify the network coverage over the Netherlands and, together with the previous and other existing arrays, provides data for imaging the crust and mantle structure with an unprecedented spatial resolution of 25 km. We described the design, development, installation, and some preliminary subsurface information delivered by the NARS-DICTUM array.

Data availability statement. Seismic data from the NSAN, NARS-NL, and DeepNL-Gronigen networks are available publicly through Orfeus Data Center (https://www.orfeus-eu.org) with the network codes NL and NR. The data from the NARS-DICTUM network will be made publicly available through the Orfeus Data Center in the future with network code NR. The earthquake catalog data are available from KNMI data portal: https://rdsa.knmi.nl/dataportal/.

Acknowledgements. This work is supported by the Dutch Research Council (NWO) DeepNL program grant number DEEP.NL.2020.010. The authors thank the Institute of Geophysics, University of Münster, Germany and the Department of Earth Sciences, Utrecht University, The Netherlands, for the seismometers used in this deployment.

References

Bonnefoy-Claudet, S., C. Cornou, P. Y. Bard, F. Cotton et al. (2006). H/V ratio: A tool for site effects evaluation. Results from 1-D noise simulations, Geophys. J. Int., 167, 2, 827-837, doi:10.1111/j.1365-246X.2006.03154.x.

Cox, B. R., T. Cheng, J. P. Vantassel and L. Manuel (2020). A statistical representation and frequency-domain window-rejection algorithm for single-station HVSR measurements, Geophys. J. Int., 221, 3, 2170-2183, doi:10.1093/GJI/GGAA119.

Dost, B. and H. W. Haak (2007). Natural and induced seismicity, in Geology of the Netherlands T. Wang, D. A. J. Btjes and J. de Jager (Eds.), Royal Netherlands Academy of Arts and Sciences, 223-239.

Furumura, T. and B. L. N. Kennett (2001). Variations in Regional Phase Propagation in the Area around Japan, B. Seismolol. Soc. Am., 91, 667-682, doi:10.1785/0120000270.

Hasselmann, K. (1963). A Statistical Analysis of the Generation of Microseisms, Rev. Geophys., 1, 177-210, doi:10.1029/RG001i002p00177.

Houtgast, R. F. and R. T. van Balen (2000). Neotectonics of the Roer Valley Rift System, the Netherlands, Glob. Planet. Change, 201, 131-146, doi:10.1016/S0921-8181(01)00063-7.

KNMI (1993). Netherlands Seismic and Acoustic Network, Royal Netherlands Meteorological Institute (KNMI) Dataset, doi:10.21944/e970fd34-23b9-3411-b366-e4f72877d2c5.

KNMI (2024). Seismic measuring stations, https://www.knmi.nl/kennis-en-datacentrum/uitleg/seismische-meetstations.

KNMI (2025). Earthquakes – complete catalogue for the Netherlands and near surrounding, Dataset, https://dataplatform.knmi.nl/dataset/aardbevingen-catalogus-1.

Kombrink, H., J. C. Doornenbal, E. J. T. Duin, M. Den Dulk et al. (2011). New insights into the geological structure of the Netherlands, Results of a detailed mapping project, Netherlands J. Geosci., Geol. Mijnb., 91, 4, 419-446, doi:10.1017/S0016774600000329.

Mcnamara, D. E. and R. P. Buland (2004). Ambient Noise Levels in the Continental United States, B. Seismol. Soc. Am., 94, 4, 1517-1527, doi:10.1785/012003001.

Nolet, G. and N. J. Vlaar (1982). The NARS Project: Probing the Earth's interior with a large seismic antenna, Terra Cognita, 2.

Paulssen, H., B. Dost and T. van Eck (1992). The April 13, 1992, earthquake of Roermond (The Netherlands), first interpretation of the NARS seismograms, Geol. Mijnb., 71, 91-98.

Paulssen, H., J. Visser and G. Nolet (1993). The crustal structure from teleseismic P-wave coda-I Method, Geophys. J. Int., 112, 15-25, doi:10.1111/j.1365-246X.1993.tb01433.x.

Peterson, J. (1993). Observation and modeling of seismic background noise, U. S. Geological Survey, Open-File Report, 93-322, doi:10.3133/ofr93322.

Ruigrok, E., P. Kruiver and B. Dost (2023). Construction of earthquake location uncertainty maps for the Netherlands, KNMI number TR-405, 158.

Trnkoczy, A., P. Bormann, W. Hanka, L. G. Holcomb et al. (2012). Site Selection, Preparation and Installation of Seismic Stations, In New Manual of Seismological Observatory Practice 2 (NMSOP-2) P. Bormann (Ed.), Deutsches GeoForschungsZentrum GFZ, doi:10.2312/GFZ.NMSOP-2_ch7.

Utrecht University – UU Netherlands (1983). The Network of Autonomously Recording Seismographs (NARS), In International Federation of Digital Seismograph Networks, http://www.geo.uu.nl/Research/Seismology/nars.html.

Van Ginkel, J., E. Ruigrok, J. Stafleu and R. Herber (2022). Development of a seismic site-response zonation map for the Netherlands, Nat. Hazards Earth Syst. Sci., 22, 1, 41-63, doi:10.5194/nhess-22-41-2022.

Vantassel, J. (2020). jpvantassel/hvsrpy: v2.0.0, doi:10.5281/ZENODO.12735911.

Visser, J. and H. Paulssen (1993). The crustal structure from teleseismic P-wave coda-II, Application to data of the NARS array in western Europe and comparison with deep seismic sounding data, Geophys. J. Int., 112, http://gji.oxfordjournals.org/.

Yudistira, T. (2015). The crustal structure beneath the Netherlands inferred from ambient seismic noise, Utrecht University.

Yudistira, T., H. Paulssen and J. Trampert (2017). The crustal structure beneath The Netherlands derived from ambient seismic noise, Tectonophysics, 721, 361-371, doi:10.1016/j.tecto.2017.09.025.

***CORRESPONDING AUTHOR: Stephen AKINREMI**,
Faculty of Geo-Information Science and Earth Observation (ITC), University of Twente, Enschede, The Netherlands
e-mail: s.akinremi@utwente.nl